Supporting Information

Machine Learning Assisted Design of Oxygen-containing Inorganic Coating Materials on Separator for Lithium Metal Anode

Chenxi Xu, [a] Teng Zhao,* [a,b,c] Ji Qian, [a,b,c] Ke Wang, [a] Tianyang Yu, [a] Wangming Tang, [a] Li Li, [a,b,c,d] Feng Wu, [a,b,c,d] and Renjie Chen* [a,b,c,d]

Corresponding authors' E-mail: Renjie Chen:chenrj@bit.edu.cn;
Teng Zhao:tz270@bit.edu.cn

a. Beijing Key Laboratory of Environmental Science and Engineering, School of Material Science & Engineering, Beijing Institute of Technology, Beijing 100081, China.

b. Innovative Research Team in High-Safety Energy Storage System and Smart Microgrids of Guangdong Province, Beijing Institute of Technology (Zhuhai), Zhuhai 519088, China

c. Shandong Key Laboratory of Advanced Chemical Energy Storage and Intelligent Safety, Advanced Technology Research Institute, Beijing Institute of Technology, Jinan 250300.

d. China.Collaborative Innovation Center of Electric Vehicles in Beijing, Beijing 100081, China

Interface reaction energy: It is calculated by constructing a pseudo-binary phase diagram, which has been used in previous studies for the interface.[1] Calculation details are as follows.

The reaction energy between lithium and coating materials was estimated by the thermodynamic approximation method. The interface can be assumed as a pseudo-binary system (A: Li, B: coating materials), equation 1:

$C_{interface}\ (c_A,c_B\ ) = \mathrm{x}c_A + (1–\mathrm{x})\ c_B$ (1)

Where x is the molar fraction of Li, and c_A and c_B are the specific composition of Li and coating materials. The total energy of pseudo-binary interface is described as the liner combination of Li and materials, equation 2. $E(c_A)$ and $E(c_B)$ are the ground state energy of Li and coating materials, respectively.

$\Delta E_{interface}\ (c_A,c_B,\ x) = \mathrm{x}E(c_A\ ) + (1–x)E(c_B\ )$ (2)

The mutual reaction energy $\Delta E_{D,mutual}\ (c_A,c_B,\ x)$ can be calculated by constructing a pseudo-binary phase diagram between Li and cotaing materials and determining the ratio (x) that result in the x most negative mutual reaction energy, equation 3:

$\Delta E_{D,mutual}\ (c_A,c_B,\ x) = \min\ 1/N[E_{eq,\ interface}\ (xc_A + (1–x)c_B\ ) – xE_D\ (c_A\ ) – (1–x)E_D\ (c_B\ )]$

$x \in [0,1]$ (3)

Here, $E_{eq,interface}$ is the reaction energy of the pseudo-binary phase, $E_D\ (c_A\ )$ and $E_D\ (c_B\ )$ are the decomposition energy of Li and coating materials. N is the number of atoms involved in the phase equilibrium used to normalization.

The Tafel curves and EIS measurements were conducted on an electrochemical workstation (CHI 660E, ChenHua Instruments Co., China). Tafel curves were conducted in the voltage range of -0.1-0.1 V with a scan rate of 0.1 mV s^{-1}. EIS data were collected in the frequency range of 100 kHz to 10 mHz with amplitude of 10 mV. Ionic conductivity was tested in a configuration of the stainless steel(SS)|separator|SS. The ion conductivity was calculated using the Equation (4):

$$\sigma = \frac{L}{R_s S} \qquad (4)$$

where L represents the thickness of the separator, Rs is determined from the EIS plot, and S denotes the area of SS electrode.

Table S1 Descriptors to predict lithium-ion conductivity

name	parameters
Elemental property attributes	Atomic Number, MendeleevNumber, AtomicWeight, MeltingT, Column, Row, CovalentRadius, Electronegativity, NsValence, NpValence, NdValence, NfValence, Nvalence, NsUnfilled, NpUnfilled, NdUnfiled, NfUnfilled, Nunfilled, Gsvolumepa, Gsbandgap, Gsmagmom, SpaceGroupNumber
Stoichiometric attributes	0-norm, 2-norm, 3-norm, 5-norm, 7-norm, 10-norm
Valence orbital shells attributes	s valence electrons, p valence electrons, d valence electrons, f valence electrons
Packing efficiency attributes	dist from 1 clusters |APE| < 0.010 , dist from 3 clusters |APE| < 0.010 dist from 5 clusters |APE| < 0.010
Temperature	T

Table S2. The performance of the four algorithms on the training set and the test set

algorithm	Best_Params	accuracy	recall score	AUC
GBDT	'classifier__learning_rate': 0.1, 'classifier__max_depth': 5, 'classifier__min_samples_split': 20, 'classifier__n_estimators': 100, 'classifier__subsample': 0.8	0.8152	0.8936	0.9125
RF	'classifier__max_depth': None, 'classifier__max_features': 'log2', 'classifier__max_samples': None, 'classifier__min_samples_leaf': 4, 'classifier__min_samples_split': 2, 'classifier__n_estimators': 50	0.8154	0.8936	0.913
SVM	'classifier__C': 0.1, 'classifier__gamma': 'scale', 'classifier__kernel': 'linear'	0.9077	0.9574	0.9291
KNN	'classifier__n_neighbors': 3, 'classifier__p': 1, 'classifier__weights': 'distance'	0.7846	0.8085	0.8079

Fig. S1 Pristine PP contact Angle test results (29°).

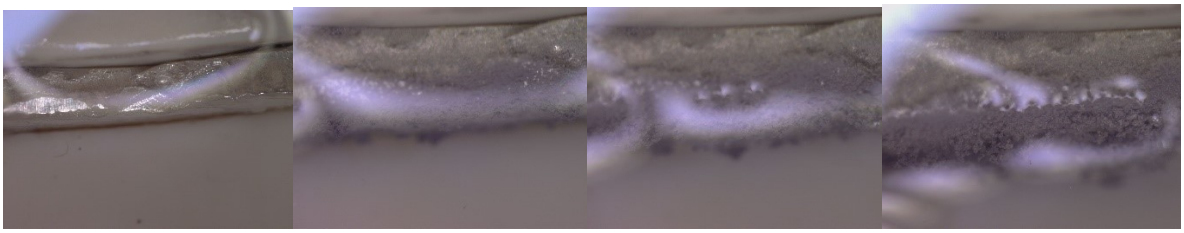

Fig. S2 In situ optical microscopy of the lithium deposition process on the anode after discharging for 0, 20, 40 and 60 min at 20 mA cm^{-2}.

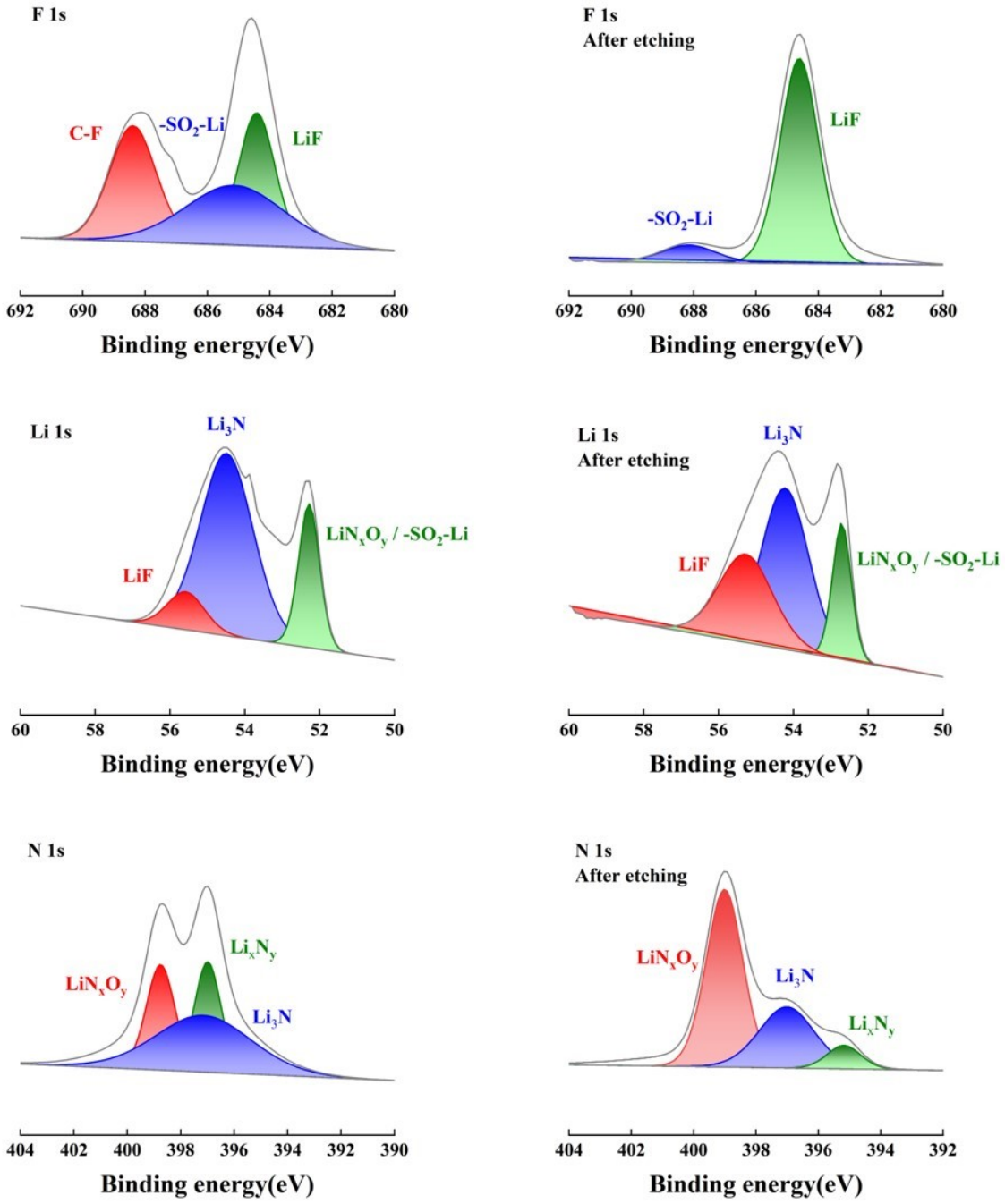

Fig. S3 XPS characterization of SEI formed on lithium metal interphase of pristine PP, including F 1s, Li 1s, and N 1s.

Reference

[1] F. Ren, Z. Liang, W. Zhao, W. Zuo, M. Lin, Y. Wu, X. Yang, Z. Gong, Y. Yang, *Energy Environ. Sci.* **2023**, 16, 2579.